Taylor & Francis
Taylor & Francis Group

Vehicle System Dynamics
International Journal of Vehicle Mechanics and Mobility

ISSN: (Print) (Online) Journal homepage: https://www.tandfonline.com/loi/nvsd20

Suspension parameters matching of high-speed locomotive based on stability/comfort Pareto optimization

Guang Li, Ruidong Wu, Xiaoxing Deng, Longjiang Shen & Yuan Yao

VEHICLE SYSTEM DYNAMICS
https://doi.org/10.1080/00423114.2021.1979602

Suspension parameters matching of high-speed locomotive based on stability/comfort Pareto optimization

Guang Li[a], Ruidong Wu[a], Xiaoxing Deng[b], Longjiang Shen[b] and Yuan Yao[a]

[a]State Key Laboratory of Traction Power, Southwest Jiaotong University, Chengdu, People's Republic of China; [b]Bogie R&D Department of CRRC Zhuzhou Electric Locomotive Co., Ltd, Zhuzhou, People's Republic of China

ABSTRACT

Suspension parameters optimisation and matching is a very important topic in the design of railway vehicles, and a reasonable combination of suspension parameters is the most powerful guarantee for safe and stable operation. However, most of the existing research about that still belongs to single-objective optimisation and pays little attention to the matching relationship between different suspension parameters, which has plenty of limitations. Therefore, the lateral stability and ride comfort of a certain type of domestic high-speed locomotive are studied and optimised through the genetic algorithm NSGA-II, to find the optimal lateral dynamic performance. It can be found that there is an obvious contradiction between linear stabilities under low-conicity and high-conicity conditions, but a strong positive correlation between low-conicity stability and lateral ride comfort in a low-conicity condition. Besides, the matching relation of the six key suspension parameters is explored employing data analysis methods, such as global sensitivity and clustering analysis, and three types of parameter combinations are proposed. In addition, the speed robustness and rail cant robustness regarding the three types of parameter combinations are analyzed, and the lateral dynamic performance characteristics of each parameter combination type are summarised.

ARTICLE HISTORY
Received 1 June 2021
Revised 31 July 2021
Accepted 4 September 2021

KEYWORDS
High-speed locomotive
suspension parameters
NSGA-II lateral stability ride comfort

1. Introduction

Lateral stability and ride comfort are two very essential evaluating indexes for the railway vehicle lateral dynamics, which must be given serious consideration in the design of high-speed locomotive. The former can ensure that locomotives can run stably and safely at a certain speed, and the latter determines whether the drivers or passengers have a good riding comfort. Generally speaking, the methods of enhancing the lateral dynamic performance of railway vehicles can be divided into two aspects. On the one hand, the application of improved structure or advanced technology can strengthen the lateral dynamic performance. In the past decades, the flexible suspension of the drive device has been widely studied as a suspension mode to improve effectively the lateral dynamic performance of

CONTACT Yuan Yao yyuan8848@163.com

railway vehicles, and this technology has already been applied to locomotives and high-speed EMU [1,2]. In addition, the advanced technology of active control and semi-active control utilised in railway vehicles has also been receiving much attention, and the research content mainly involves the improvements of ride comfort and hunting mode [3–8]. Currently, the semi-active technology manipulated in the secondary suspension of railway vehicles has been widely adopted in Japan, which is loaded on both existing lines and Shinkansen. However, the application of active control technology in railway vehicles is relatively few, only tilting trains [9].

On the other hand, suspension parameters optimisation can be another resultful and practical way to improve the lateral dynamic performance of railway vehicles, and there are some researches about suspension parameters optimisation. Suarez and his research team utilised different icons to characterise the influence of each parameter, which includes the inertial parameters of the vehicle structure, primary horizontal stiffness, secondary vertical stiffness and damping, but the applied method is still a single parameter change [10]. In actual operation, railway vehicles are demanded to meet multiple lateral dynamic performances, such as the lateral stability and ride comfort on straight track as well as curve passing ability, but these performance indexes constantly have contradictory requirements for suspension parameters. Therefore, multiple dynamic performances should be taken into account and compromised when the suspension parameter of railway vehicles is optimised [11–13]. Multi-objective optimisation is widely applied in the suspension parameter design of railway vehicles, which is an effective method to solve practical engineering problems. And the genetic algorithm is ordinarily utilised in the multi-objective optimisation inasmuch as it shows significant advantages over most intelligent search algorithms, such as the highest probability of global optimisation [14]. Johnsson and others utilised GAs to optimise the passive damping elements of the bogie suspension, whose optimisation results can improve the safety and comfort of railway vehicles [15]. He and McPhee proposed a method that can effectively deal with the conflicting requirements of railway vehicle design by GAs. They also used genetic algorithms to solve the optimisation of the curve passing performance problem of a railway vehicle model with 21 degrees of freedom [16,17]. Seyed established a railway vehicle model with 50 degrees of freedom, and the global sensitivity analysis had been carried out based on the multiplicative dimensional reduction method(M-DRM). Then, the Pareto optimisation problem of the wear and comfort of the bogie suspension was solved through GAs, and the running speed of the vehicle on the curve was also improved [18–20]. For high-speed train, Yao Yuan put forward the concept of robust stability aiming at the hunting mode, and optimised several key suspension parameters simultaneously through the improved non-dominated sorting genetic algorithm NSGA-II, summarising the suspension parameters matching types [21,22]. With the academic research about the suspension parameter optimisation above, we can conclude that most of the existing investigation focuses on optimising the lateral dynamic performance of railway vehicles, but lacks in the discussion of matching relationship between suspension parameters.

In the subsequent sections, the dynamic modeling regarding a certain type of high-speed electric locomotive (Bo-Bo) with 90 degrees of freedom is established by multibody dynamics software SIMPACK [23], and the calculation and evaluation methods of vehicles system linear stability and lateral ride comfort are introduced. Then, three optimisation objects and six suspension parameters designed are given, and the genetic algorithm NSGA-II is utilised to conduct the multi-objective optimisation through the MATLAB/ SIMPACK co-simulation interface. Finally, Concerning lateral stability and ride comfort, the matching relation between the six suspension parameters is explored utilising Sobol sensitivity and K-means clustering analysis. It should be noted that the matching law of the suspension parameters obtained in the study is just the authors' superficial understanding and cognition, which may be immature and imperfect. It is hoped that the research result can provide certain theoretical support for the suspension parameter design of railway vehicles.

2. Dynamic modeling

This section introduces the composition of the locomotive dynamic model established by SIMPACK, and presents the track condition and track irregularities. Besides, the wheel-rail contact geometry of the dynamic model is described in detail, and the influence of the rail cant variation on the wheel-rail geometry is analyzed. Finally, the accuracy of the established dynamic model is verified.

2.1. High-speed locomotive dynamic model

Based on the structure and suspension parameters of high-speed electric locomotive (Bo-Bo) provided by CRRC Zhuzhou Electric Locomotive Co., Ltd, the high-speed locomotive dynamic model with 90 DOFs is established by SIMPACK and shown in Figure 1. The dynamic model consists of 25 rigid bodies including a carbody, two bogie frames, four wheelsets, four motors, four hollow shafts, two traction rods, and eight rotary arm bodies of axle-boxes. Several rigid bodies including carbody, bogie frame, wheelset, and motor have six degrees of freedom (DOFs) in space. Each hollow shaft owns three DOFs that include yaw, rolling and lateral around the wheelset respectively, every traction rod allows pitch and yaw DOFs along the carbody, and each rotary arm of axle-boxes merely has a single rotation DOF along the wheelset axle. The wheel-rail surfaces are created based on the JM3 tread and CN60 rail surface, and the gauge is 1.435 m. Besides, the wheel-rail tangential force is calculated by the FASTSIM algorithm [24], where the value of Kalker coefficient is set to 1, and the elastic contact ellipse characteristics are approximated using an equivalent-elastic contact search procedure in SIMPACK.

The suspension components of the high-speed locomotive are presented as follows. The primary suspension is between the bogie frame and the wheelset, which involves the axle box spring and rotary arm. The former affords vertical stiffness, and the latter mainly provides longitudinal and lateral stiffness. The secondary suspension acts between the carbody and the bogie frame, including flex-coil spring, yaw damper, secondary lateral damper, and secondary vertical damper. Moreover, the anti-rolling torsion bar and the secondary lateral stopper are considered. Besides, the suspension mode of the drive device adopts the flexible suspension that every motor is suspended on the bogie frame through one hanging-ear and two hanger rods. In addition, the nonlinear characteristics are considered in the modeling of all dampers and the stop components.

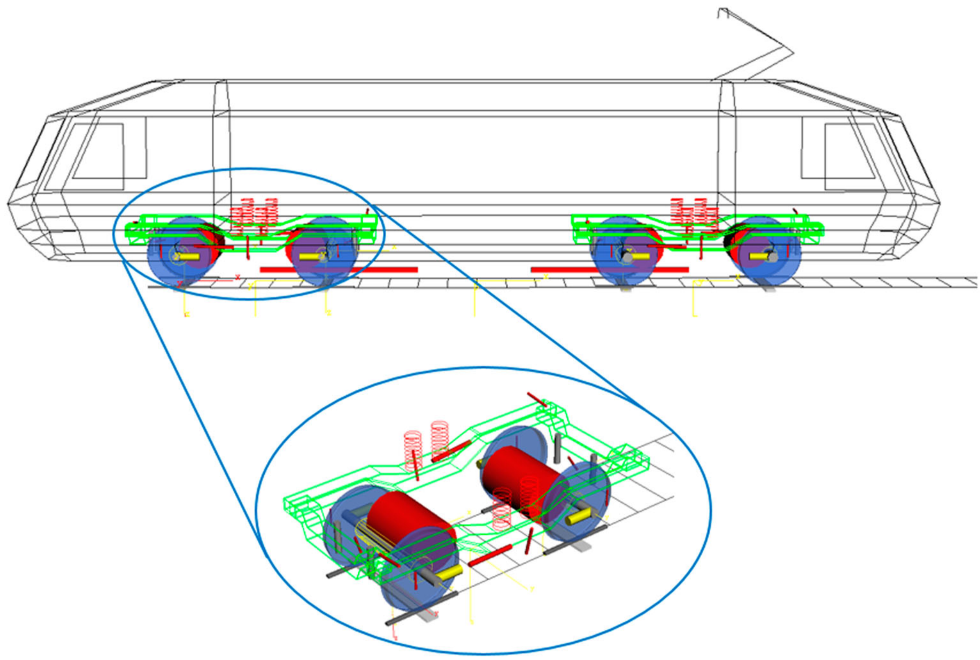

Figure 1. High-speed locomotive dynamic model.

2.2. Track condition and irregularity

Track conditions and irregularities are quite important boundary conditions for railway vehicles, which have a decisive influence on the dynamic performance of railway vehicles. In reality, railway tracks are composed of multiple types of straight lines, curves, and special track sections, and railway vehicles will show different dynamic responses when passing through these tracks. Here, the dynamic performance of the locomotive on the straight-line section is only studied.

For track irregularities, the Wuhan Guangzhou High-speed Rail track spectrum [25] is chosen, which was measured by track geometry inspection car from Wuhan-Guangzhou high-speed rail, and the measured track spectrum is widely employed in the dynamic simulation for Chinese railway vehicles. Moreover, it should be noted that Wuguang High-speed Rail measured track spectrum will be utilised in all time-domain simulations below. In SIMPACK, the Wuguang High-speed Rail track spectrum is read in the form of a TRE file, and loaded on the track in the light of the Track-Related track irregularity method that track irregularities are defined in the four directions lateral, vertical, roll and gauge, referring to both rails at once.

2.3. Wheel-rail contact geometry

The wheel-rail contact geometry is one of the most important dynamic parameters of railway vehicles, which is affected by the wheel treads, the rail profile and the rail cant in the actual track [26], and the equivalent conicity is usually employed to represent the wheel-rail contact geometry. Also, the inappropriate equivalent conicity will deteriorate vehicle lateral

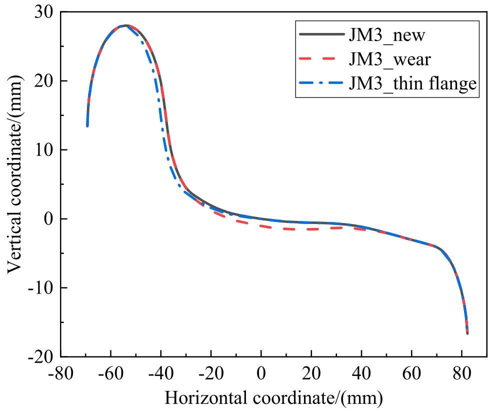

Figure 2. JM3 tread profile with different status.

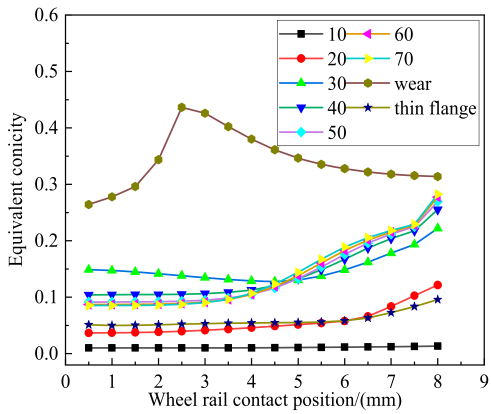

Figure 3. The equivalent conicity curves.

dynamic performances. For example, because the wheel-rail contact equivalent conicity is too small, the electric locomotives (Bo-Bo) in China have emerged lateral swaying of the carbody on certain track sections, which has seriously affected the ride comfort of drivers and passengers [27]. This is due to the geometry design of thin flange JM3 profile or the larger rail cant on part of the track. Figure 2 shows the JM3 tread profiles under the status of new, wear and thin flange.

The definition of rail cant is a certain slope of the inward inclination of railway tracks, whose purpose is to make the wheels and rails cooperate to obtain a good wheel-rail contact geometry. Countries have various regulations on the value of rail cant: the standard value of rail cant is 1/40 in China, and the standard value of rail cant commonly is set to 1/40 or 1/20 in Europe, but the standard value of rail cant is 1/30 in a few countries [28]. Nevertheless, the value of rail cant in the actual track is variable and unequal to the specified standard value generally, which is owing to construction imperfections, usage in service, and changes on the track substructure resulting from temperature effects or soil motion [29]. The variation range of rail cant is from 1/70–1/10 during a certain straight track in China, which is measured by the field test [27]. The equivalent conicity curves

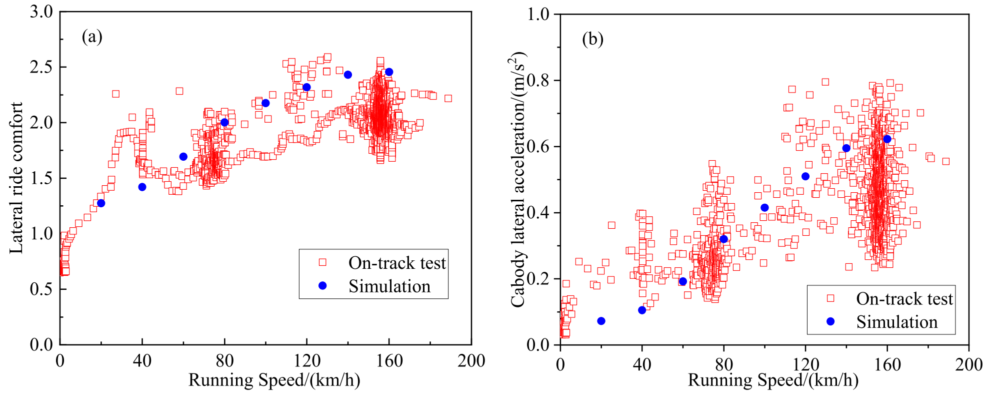

Figure 4. The comparison between the on-track test and simulation results.

of JM3 tread under different values of rail cant, JM3 wear tread and thin flange JM3 profile under the domestic standard rail cant are shown in Figure 3. It can be drawn that the rail cant variation can affect the equivalent conicity, and the larger rail cant significantly reduces the equivalent conicity regarding the JM3 new tread, but the smaller rail cant has little influence on the equivalent conicity. Besides, the equivalent conicity of the JM3 wear tread under 1/40 rail cant is evidently larger, which is defined as the high-conicity condition. Moreover, the equivalent conicity curve of the JM3 new wheel under the rail cant 1/20 is basically the same as the equivalent conicity curve under the JM3 thin flange, and the equivalent conicity is small. Thus, the JM3 new tread with the values of rail cant 1/20 and 1/40 are defined as the low-conicity condition the normal-conicity condition respectively in the following research.

2.4. Model validation

In order to verify the accuracy of the established high-speed locomotive dynamic model, the lateral ride comfort of the high-speed locomotive under the normal-conicity condition is calculated and compared with the on-track test during the Kunming-Qujing Section. The comparison result of the lateral ride comfort and carbody lateral acceleration between the on-track test and simulation is shown in Figure 4, where the horizontal axis represents the vehicle running speed. It can be found that the lateral ride comfort and carbody lateral acceleration of simulation results are basically the same as the on-track test results, proving the accuracy and rationality of the established dynamic model.

3. Evaluation index

The definition, calculation and evaluation methods of linear stability index and lateral ride comfort index are introduced in this section.

3.1. Linear stability

The lateral stability of railway vehicles system consists of linear stability and nonlinear stability. The loss of linear stability is generally described by the linear critical speed presented in the root locus curve, and nonlinear stability is commonly represented by the nonlinear critical speed. Polach conducted a comparable evaluation of the linear and nonlinear stability of railway vehicles [30,31], and pointed out that linear stability analysis is still useful and important for vehicle design, even if nonlinear stability analysis is more accurate for the stability evaluation of railway vehicles. Considering that the calculation workload of the nonlinear stability is relatively larger, the linear stability analysis is adopted to represent the lateral stability of railway vehicles.

$$\eta = a + bi \tag{1}$$

$$f = |b|/2\pi \tag{2}$$

$$\zeta = a/\sqrt{a^2 + b^2} \tag{3}$$

The root locus method is employed to calculate the linear stability of the railway vehicle system, whose essence is to solve eigenvalues and eigenvectors of the Jacobian matrix of the vehicle linear system. Specifically, 'η' is assumed to be a certain eigenvalue value of the Jacobian matrix, which is a plural and shown in the Eq. (1). The symbols 'a' and 'b' are the real part and the imaginary part of the eigenvalue respectively, and the symbol 'i' is the imaginary unit. In Eq. (2), the modal vibration frequency f is the absolute value of the imaginary part of the eigenvalue, reflecting the vibration of the vehicle system. As Eq. (3) shows, the modal vibration-damping ratio ζ is the ratio of the real part to the modulus of the eigenvalue, which is defined as the linear stability index, standing for the lateral stability of the vehicle system, and the vehicle system is regarded to be stable when the value of linear stability index ζ is less than 0. When the root locus is calculated by SIMPACK, all force elements with nonlinear characteristics in the dynamic model are linearised.

3.2. Lateral ride comfort

Currently, the ride comfort of rolling stock is the feeling of the driver or passengers on the running quality, and the Sperling index is an internationally recognised method to evaluate the ride comfort of rolling stock. Generally speaking, the Sperling index includes the lateral ride comfort index and vertical ride comfort index. The lateral ride comfort index is only studied here, and the calculation formula of this index is as follows [32]:

$$W_y = 3.57 \sqrt[10]{\frac{A_y^3}{f} F(f)} \tag{4}$$

In Eq. (4), W_y is the lateral ride comfort index, A_y is the amplitude in the frequency domain derived from an FFT analysis of the measured lateral acceleration, where the measurement location is usually the carbody floor, and f is the corresponding frequency. $F(f)$ is the frequency correction coefficient, which can be obtained by checking the frequency correction coefficient table from GB/T5599-2019. It is worth noting that total simulation time is set to 11.25s and the integration time step is set to 10^{-6}s. After calculating the index W_y, it can be evaluated through the grading table of locomotives lateral ride comfort index. When the index W_y is less than 2.75, the lateral ride comfort level of the locomotive is deemed to be excellent, and the lateral ride comfort of the high-speed locomotive is required to reach an excellent level generally.

4. The multi-objective optimal

The description and general solving methods of the multi-objective optimisation problem are introduced in this section. In addition, the optimisation objectives and design parameters as well as the optimisation algorithm and route are presented.

4.1. Multi-objective optimisation problem description

In many practical engineering problems, multi-objective optimisation problems are very common and play a very important role in the problem optimisation. Compared with the single-objective optimisation problem, multi-objective optimisation problems are more complicated and difficult to find a solution to make all objectives optimal. In other words, when one solution is the best for one optimisation objective, it is not the best or even the worst for other optimisation objectives, because optimisation objectives can have different requirements for design parameters. Accordingly, the solutions of the multi-objective optimisation problem are ordinarily a set of solutions that cannot be compared regarding to various optimisation objectives, which can be called non-dominated solutions or Pareto optimal solutions. This is the essential distinction between the multi-objective and single-objective optimisation.

Generally Speaking, the mathematical form of multi-objective optimisation problem can be described as follows:

$$\left.\begin{array}{c} \min \quad F(x)=[f_1(x), f_2(x), \cdots f_m(x) \cdots, f_M(x)] \\ s.t. \quad g_i(x)\leq 0 \quad (i=1,2,\cdots,p) \\ h_j(x)=0 \quad (j=1,2,\cdots,q) \\ find \quad design\,\text{variable} \quad x=[x_1,x_2,\cdots x_n,\cdots,x_N] \\ x_n\_\min \leq x_n \leq x_n\_\max \quad (n=1,2,\cdots,N) \end{array}\right\} \tag{5}$$

In Eq. (5), x represents the design variable, $f(x)$ is the objective function, $F(x)$ is the objective vector, $g(x)$ is the inequality constraint, and $h(x)$ is the equality constraint, The subscripts i and j are the number of inequality and equality constraints, respectively, and the subscripts m and n are the number of objective functions and design variables, and M and N is the total number of optimisation objectives and design variables. x_n_min and x_n_max are the lower and upper limits of the optimised scope corresponding to the nth design variable.

Usually, there are two methods to handle the multi-objective optimisation problem. The first method is to convert the multi-objective problem into a single-objective problem by the weighting and summation, as shown in Eq. (6), but it is extremely difficult to determine the suitable weighting coefficient w_n. Besides, when the dimensions of multiple optimisation objectives vary greatly, it is easy to cause poor robustness in the converted single-objective optimisation problem. The second method is to utilise the optimisation algorithm to directly figure out the multi-objective optimisation problem, whose advantage is obtaining a Pareto solution set containing plenty of effective information, but the disadvantage is the poor calculation efficiency and only suitable for solving the optimisation problem with $2\sim5$ objectives. In this paper, the second method is selected to solve the multi-objective optimisation problem.

$$\min \quad F(x)=w_1f_1(x)+w_2f_2(x) \quad +\cdots+w_nf_n(x) \tag{6}$$

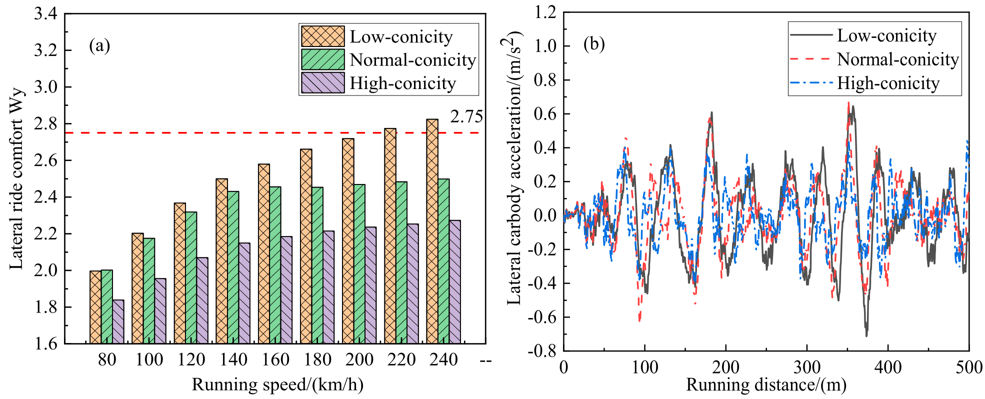

Figure 5. Lateral ride comfort indexes and carbody accelerations under three condtions.

Table 1. Optimisation indexes and working condition setting.

Index	Calculation condition v (km/h)	conicity	Wheel tread	Rail cant	Description
ζ_{low}	160	0.04	JM3_new	1/20	Low-conicity stability index
ζ_{high}	160	0.4	JM3_wear	1/40	High-conicity stability index
W_y	160	0.04	JM3_new	1/20	Lateral ride comfort index

4.2. Optimisation objectives and design parameters

The linear stability and lateral ride comfort are chosen as optimisation objectives, which is called the Stability/Comfort optimisation. For the linear stability, both the low-conicity and high-conicity conditions are considered in the optimisation, which is because the linear stabilities under the two conditions are generally contradictory and determined to be satisfied in the design of the high-speed locomotive simultaneously. Regarding the lateral ride comfort, the lateral ride comfort indexes of the high-speed locomotive under low-conicity, normal-conicity and high-conicity conditions are calculated and compared. The results of the lateral ride comfort index W_y under the three simulation conditions are shown in Figure 5(a), and Figure 5(b) is the comparison result of lateral carbody accelerations under the three conditions when the running speed is 160 km/h. It can be drawn that the lateral ride comfort under the low-conicity condition is the worst, the lateral ride comfort under the high-conicity condition is the best, which is consistent with research conclusions obtained by other scholars through numerical simulation and on-track test [33, 37]. Thus, the lateral ride comfort under the low-conicity condition should be taken into account in the optimisation. The optimisation indexes of three objectives are represented by ζ_{low}, ζ_{high} and W_y, and the specific working condition settings are shown in Table 1.

The design parameters include primary and secondary suspension parameters, and the former includes the primary longitudinal stiffness *kpx* and lateral stiffness *kpy*. The secondary suspension parameters contain the damping of yaw damper *csx*, the yaw damper series stiffness *kncsx*, the damping of secondary lateral damper *csy* and the secondary lateral damper series stiffness *kncsy*. The optimisation ranges are shown in Table 2, which is decided based on the authors' years of engineering experience in rolling stock research.

Table 2. Design parameters and optimisation ranges.

Parameters	Design ranges	Description
kpx	$10 \sim 50$(kN/mm)	primary longitudinal stiffness
kpy	$2 \sim 8$(kN/mm)	primary longitudinal stiffness
csx	$200 \sim 1000$(kN s/m)	yaw damper damping
kncsx	$10 \sim 50$(kN/mm)	series stiffness of yaw damper damping
csy	$20 \sim 50$(kN s/m)	secondary lateral damper damping
kncsy	$10 \sim 50$(kN/mm)	series stiffness of secondary lateral damper damping

4.3. *Optimisation algorithm and route*

The genetic algorithm NSGA-II is a very effective optimisation algorithm for solving multi-objective optimisation problems, which can not only greatly improve computational efficiency but also maintain population diversity. Therefore, the NSGA-II algorithm is adopted as the optimisation algorithm. The optimisation direction is to obtain smaller values of the three optimisation objectives including ζ_{low}, ζ_{high} and W_y simultaneously, as shown in Eq. (7). Moreover, the smaller the value of the optimisation objective, the better the corresponding dynamic performance of the high-speed locomotive. Because W_y is calculated through time-domain simulation during the optimisation process, the computing time is relatively larger. The population size is set to 2000, and the generation number is set to 6. Besides, the crossover probability and mutation probability are set to 0.8 and 0.2 respectively, and the parallel calculation is also enabled.

$$\min\{\zeta_{low}, \zeta_{high}, W_y\} \tag{7}$$

The NSGA-II algorithm is implemented in MATLAB, but the establishment and analysis of the high-speed locomotive dynamic model are completed by SIMPACK. So, it is very inevitable to connect MATLAB and SIMPACK to accomplish the optimisation process. In this paper, the co-simulation method utilised is editing and executing the SIMPACK script language through MATLAB to achieve the purpose of controlling the dynamic model calculation and optimisation. The SIMPACK script languages consist of pre-processing language.sjs and post-processing language.qs, whose functions are to perform calculations and obtain calculated results respectively. The concrete co-simulation route is shown in Figure 6, and the optimisation process will be terminated until the result converges or reaches the prescribed maximum iteration number.

5. Results and analysis

The Pareto frontier of Stability/Comfort optimisation is obtained, and the matching laws between parameters are studied and given. Moreover, three types of parameter combinations are proposed and the corresponding lateral dynamic performance characteristics are summarised.

5.1. *Pareto frontier results*

The Stability/Comfort Pareto frontier is shown in Figure 7(a). The abscissa and ordinate axes represent low-conicity stability ζ_{low} and high-conicity stability ζ_{high} respectively, and

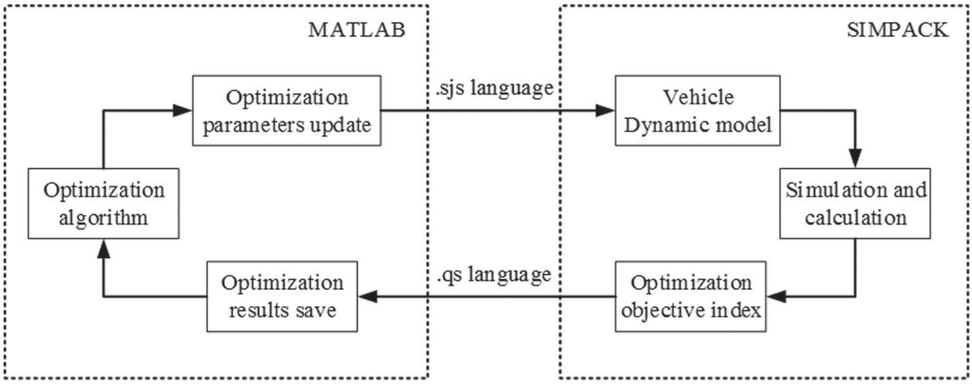

Figure 6. The route diagram of MATLAB/SIMPACK co-simulation.

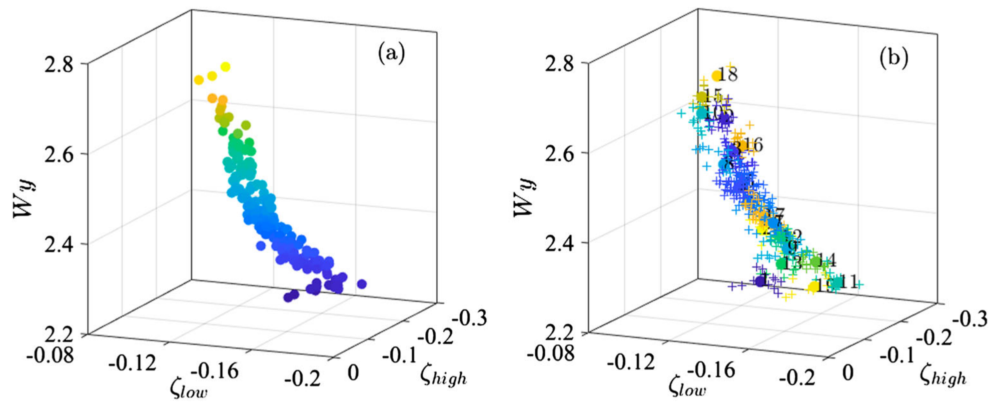

Figure 7. Stability/Comfort Pareto frontier and the Cluster analysis.

the vertical axis indicates the lateral ride comfort W_y. Besides, the colour depth also represents the W_y, where the darker colour indicates that the lateral ride comfort is better. It can be drawn that there is a negative correlation trend between ζ_{low} and ζ_{high}, but a positive correlation trend between ζ_{low} and W_y. That is, when the low-conicity stability of the high-speed locomotive is better, the lateral ride comfort is better as well, but the high-conicity stability is poor.

Figure 8 depicts the distribution of design parameters regarding W_y of Pareto frontier, and the combinations of the design parameters are regarded as Pareto sets. The abscissa axis represents the lateral ride comfort W_y, and the ordinate axis of each subgraph stands for one design parameter. It can be found that there is a strong correlation between W_y and the three suspension parameters including *csx*, *csy*, *kncsx*. Specifically, smaller values of *csx*, *csy* and *kncsx* benefit the lateral ride comfort, and it seems that the influence of *csx* is dominant. However, there is no obvious relationship between the remaining three suspension parameters and W_y. Moreover, the optimisation results show that the distribution of *kpx* is concentrated in the range of 15～20kN/mm, *kpy* can be arbitrarily adopted between 3～7kN/mm, and *kncsy* can be selected casually during 10～40kN/mm.

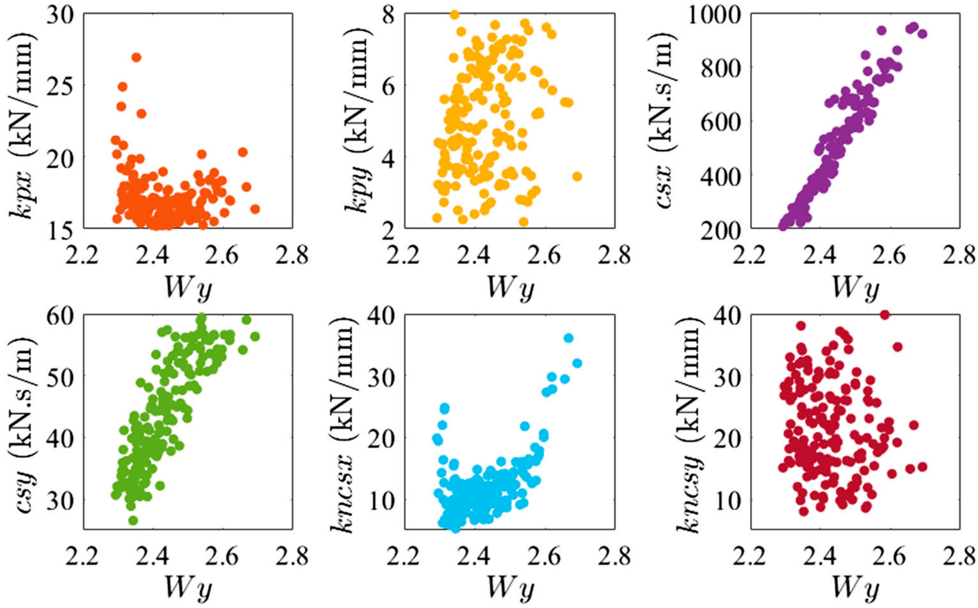

Figure 8. The distribution of design parameters regarding W_y of Pareto frontier.

5.2. Global sensitivity analysis

In order to quantitatively analyze the relationship between optimisation objectives and design parameters, and find the design parameters which greatly influence the optimisation objectives, the global sensitivity analysis is conducted. Generally, global sensitivity analysis methods include the FAST method, OAT method and Morris method, etc [34]. Here, the method of Sobol sensitivity analysis is utilised [35], whose key features are analyzing the sensitivity from the perspective of variance decomposition and quantifying the uncertainty of input and output in the form of the probability distribution. In addition, the advantages of this method are that interaction and nonlinear response can be considered, and the sensitivity analysis results are robust and reliable. The concrete solution process of the Sobol sensitivity index is as follows:

Build the model represented by a function:

$$y = \varphi(x) = \varphi(x_1, x_2, \ldots, x_n) \tag{8}$$

Where $x = (x_1, x_2, \ldots, x_n)$ stands for the model input (i.e. design parameters), y represents the mode input (i.e. optimisation objectives). The subscript n is the number of input variables.

The function φ is decomposed into summands of increasing dimensionality as:

$$\varphi(x) = \varphi_0 + \sum_{i=1}^{n} \varphi_i(x_i) + \sum_{1\le i<j\le n} \varphi_{i,j}(x_i, x_j) + \ldots + \varphi_{1,\ldots,n}(x_i, \ldots, x_n) \tag{9}$$

With φ_0 representing a constant, it is proved that the decomposition is unique and all decomposition can be obtained by multiple integrals, which is called the decomposition of $\varphi(x)$.

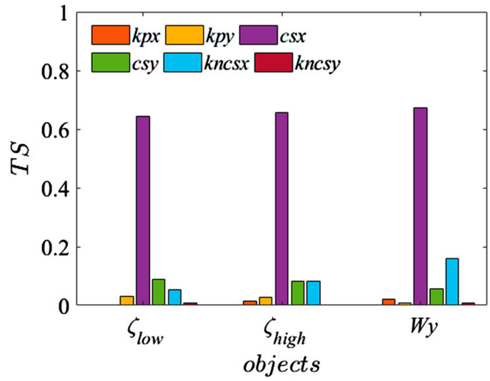

Figure 9. Global sensitivity analysis results.

The total variance D and the s order partial variance $D_{i_1,i_2,\ldots,i_s}$ of x_i can be defined as Eq. (10) and Eq. (11) separately. Where $1 \le i_1 < \ldots < i_s \le n$ and $s = 1,2,\ldots,n$.

$$D = \int \varphi^2(x)dx - \varphi_0^2 \tag{10}$$

$$D_{i_1,i_2,\ldots,i_s} = \int_0^1 \ldots \int_0^1 \varphi^2_{i_1,i_2,\ldots,i_s}(x_{i_1}, x_{i_2}, \ldots, x_{i_s})dx_{i_1}dx_{i_2}\ldots dx_{i_s} \tag{11}$$

The s order sensitivity index $S_{i_1,i_2,\ldots,i_s}$ and total sensitivity index TS_i of x_i are defined as Eq. (12) and Eq. (13) individually.

$$S_{i_1,i_2,\ldots,i_s} = \frac{D_{i_1,i_2,\ldots,i_s}}{D} \tag{12}$$

$$TS_i = S_{i_1} + S_{i_1,i_2} + \ldots + S_{i_1,i_2,\ldots,i_n} \tag{13}$$

According to the above method, the global sensitivity analysis between six design parameters and three optimisation objectives is carried out, and the total sensitivity index TS is selected as the sensitivity evaluation index, as shown in Figure 9. The horizontal axis represents the three optimisation objectives, which are low-conicity stability index ζ_{low}, high-conicity stability index ζ_{high} and lateral ride comfort index W_y, and the vertical axis is the total sensitivity index TS. It can be concluded that the three optimisation objectives are more sensitive to *csx*, *csy* and *kncsx*, but insensitivity to *kpx*, *kpy* and *kncsy*. In other words, when values of *csx*, *csy* and *kncsx* change, the lateral stability and ride comfort of the locomotive fluctuate greatly, while values variation of *kpx*, *kpy* and *kncsy* have almost no effect on the three optimisation objectives.

5.3. Parameters matching analysis

Since it is hard to directly analyze large amounts of the Pareto frontier data in Figure 7, the Clustering method is utilised to process the Pareto frontier data. K-means Clustering is a very effective data processing method with many practical applications, whose core idea

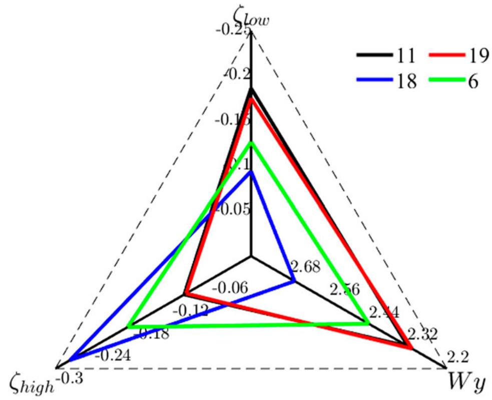

Figure 10. Objective values of four cluster centres.

is to divide data objects into different clusters through iteration to minimise the objective function [36]. Also, the distribution of the obtained clusters is generally compact and independent. Therefore, the Pareto frontier data is processed through the standardising and K-means clustering method based on spatial distance, where the number of cluster centres is set to 20. The data processing result shows that the obtained cluster centres are evenly distributed in the Pareto frontier, as shown in Figure 7(b).

For further analysis, the four representative clusters were selected from 20 clusters, namely Clusters 11th, 18th, 19th, and 6th. The optimisation objective values corresponding to the four clusters are shown in Figure 10, and the three coordinate axes in the radar chart represent the three optimisation objectives ζ_{low}, ζ_{high}, and W_y. The farther the coordinate axis from the axis intersection centre in the radar chart is, the smaller the objective value is, which means the better objective performance. It is clear that the objective value of ζ_{low}, ζ_{high}, and W_y corresponding to Clusters 11th, 18th and 19th are the smallest, respectively. The Cluster 6th is a typical parameter set that takes into account the trade-off of the three objectives, where the three dynamic performances are in balance.

Figure 11 is an axis-box diagram reflecting the distribution of six suspension parameters corresponding to the selected four clusters. In each axis-box in Figure 11, the upper and under black bars '-' represent the maximum and minimum values of the suspension parameter in the cluster area. Also, the upper and under blue bars '-' indicate the upper and lower quartile of the parameter in the corresponding cluster area, and the red bar '-' in the middle stands for the median of the parameter in the corresponding cluster area. Besides, the red symbol '+' represents the abnormal value of the parameter in the cluster area. It can be drawn that *kpx*, *kpy* and *kncsy* have no obvious influence on the lateral stability and ride comfort, which can also be confirmed from the global sensitivity analysis in section 5.2. For Clusters 11th and 19th, a smaller *csx*, *csy* and *kncsx* is adopted, where the corresponding low-conicity stability and lateral ride comfort are better, and the suspension parameter combination mode is defined as Type *Small*. Regarding Cluster 18th, the suspension parameter combination mode with a larger *csx*, *csy* and *kncsx* is adopted and defined as Type *Large*, where the high-speed locomotive has a better high-conicity stability, but the low-conicity stability and lateral ride comfort are worse. For Cluster 6th, the adopted values of *csx*, *kncsx* and *csy* are moderate, and the three objective performances

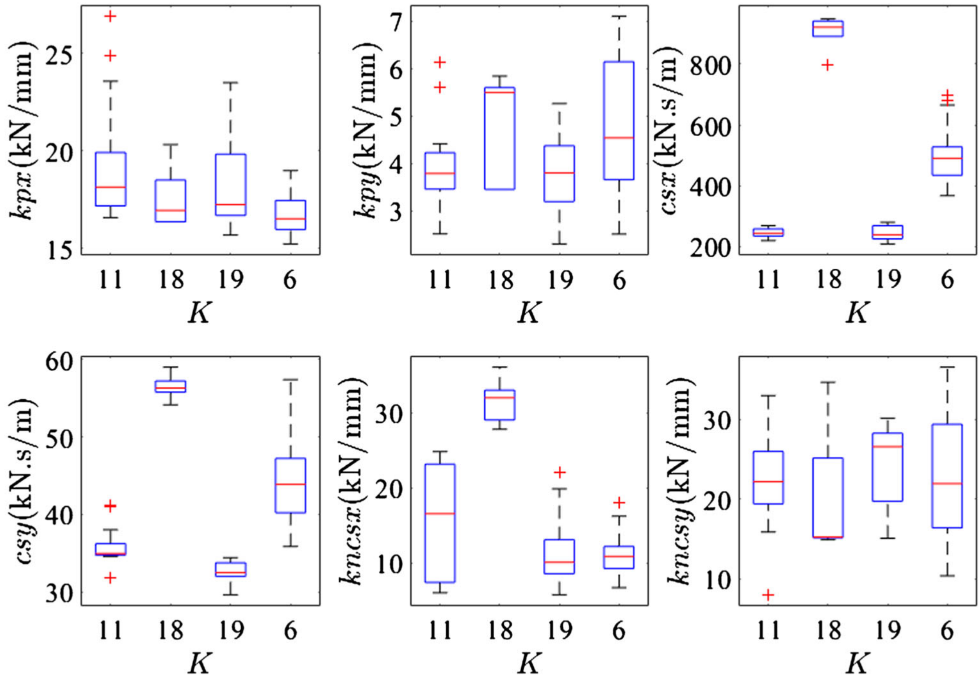

Figure 11. Suspension parameters distribution of the four clusters.

are comprised, where the parameter combination mode is called Type *Medium* and often employed in the suspension parameter design of high-speed locomotives.

5.4. Robustness analysis

5.4.1. Speed robustness

In order to analyze and compare the resistance ability of lateral stability versus vehicle running speed from the perspective of linear stability, when the suspension parameter combination corresponding to the four clusters are adopted orderly, the root locus of the high-speed locomotive with the variation of running speed is analyzed. The speed root locus curves under the low-conicity condition are shown in Figure 12, and each subgraph represents the speed root locus curve of the high-speed locomotive employing the parameter combination corresponding to one cluster. Every root locus curve is composed of 17 groups of characteristic roots with the speed range of 80 $\sim$ 400 km/h, and each '+' implies a corresponding mode under a certain speed. The larger the symbol '+' indicates that the corresponding speed is higher. The abscissa axis represents the mode damping ratio, which is indicated by the symbol 'ζ', and the ordinate axis represents the mode vibration frequency with damping. The relationship between the value of ζ and the vehicle system linear stability has been illustrated in Section 3.1, and there is the stable region when the value of damping ratio is below zero, on the contrary, the other side is the unstable region. Mostly, the bogie hunting mode [37] with a low-frequency (1–5 Hz) determines the railway vehicle hunting critical speed, and the bogie hunting frequency will increase in the high-conicity

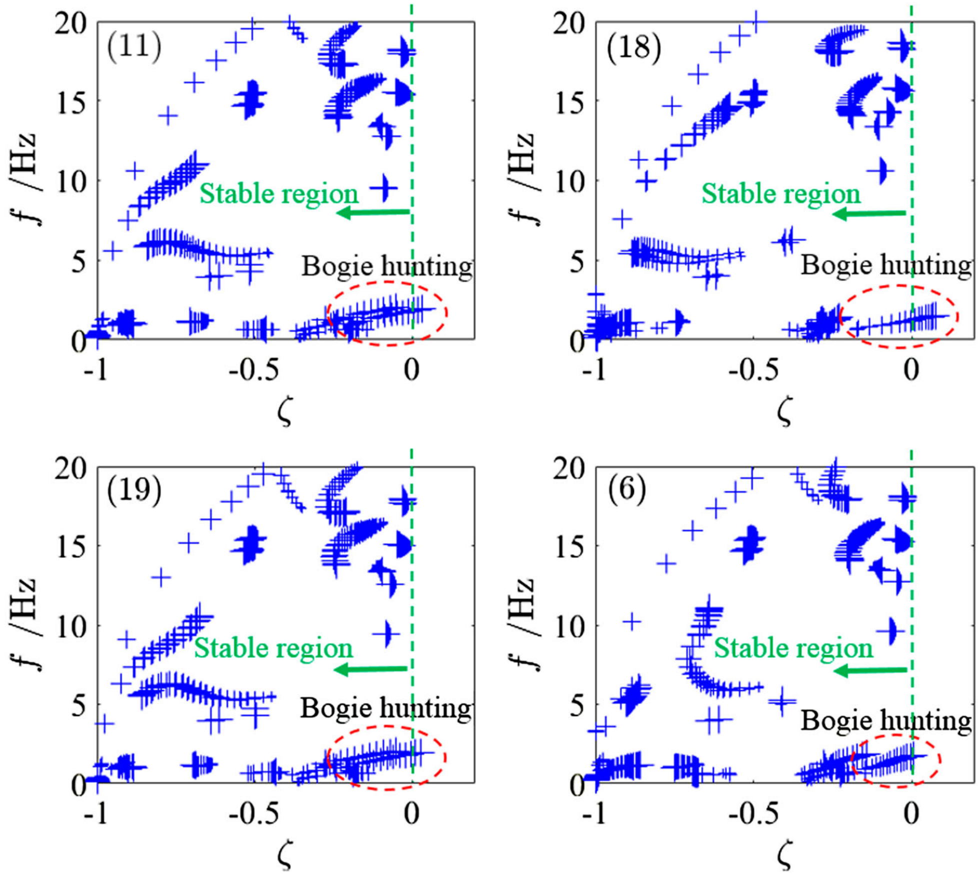

Figure 12. The speed root locus under the low-conicity condition.

condition. In Figure 12, the bogie hunting modes during the full calculated speed range are marked by red dotted circle.

As Figure 12 shows, when the wheel-rail contact equivalent conicity is small, the linear stability of the high-speed locomotive corresponding to the Cluster 11th or 19th is excellent at lower speeds, but decreases significantly with the increase of running speed. In other words, the speed robustness of linear stability is poor when the high-speed locomotive adopts the suspension parameter combination of the Cluster 11th or 19th, and the speed robustness of locomotive adopting the parameter combination of Cluster 18th is also weak. However, when the high-speed locomotive employs the suspension parameter combination of Cluster 6th, the speed robustness of linear stability is strong. Besides, it can also be found that the high-conicity linear stabilities of the high-speed locomotives corresponding to the four clusters are all better.

In short, only if the high-speed locomotive adopts the suspension parameter combination of Type *Medium*, the speed robustness of linear stability under the low-conicity condition is good. Regardless of whether the high-speed locomotive adopts the parameter combination of Type *Small* or Type *Large*, the speed robustness of low-conicity linear stability will be poor. For the high-speed locomotive corresponding to the four selected

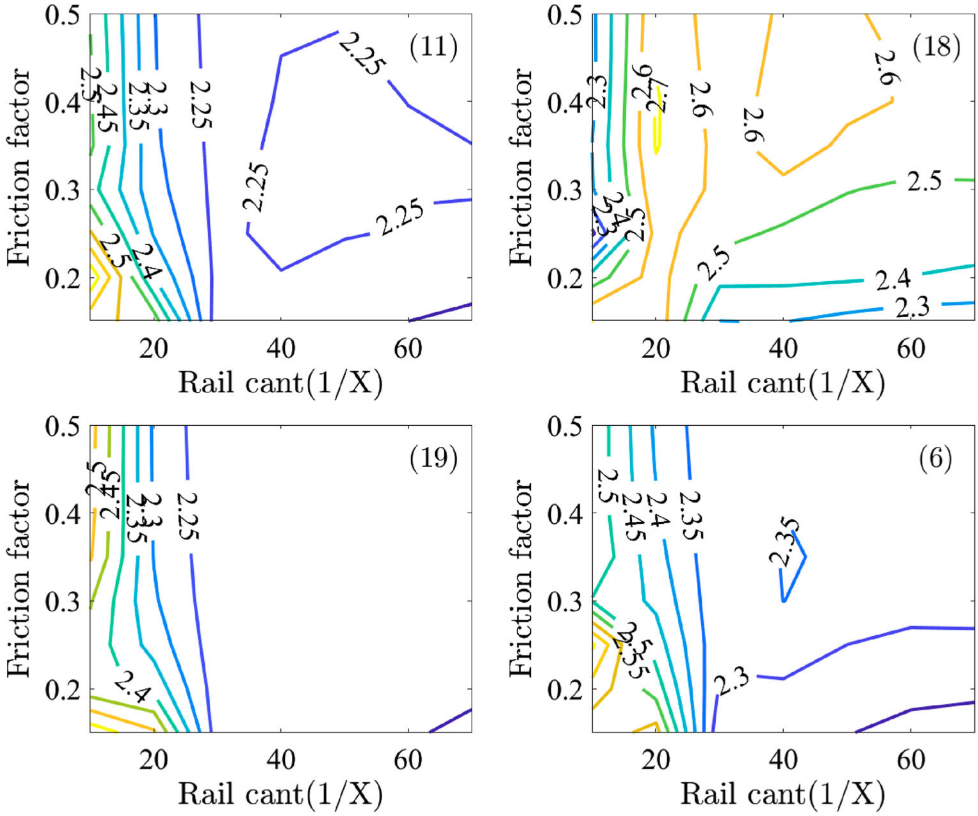

Figure 13. Lateral ride comfort index under different rail cant and friction factor when the locomotive employs the parameter combination of Cluster 11th, 18th, 19th or 6th respectively.

clusters under the high-conicity condition, the speed robustness of linear stability is all good.

5.4.2. Rail cant robustness

In the actual operation of high-speed locomotives, the value of the rail cant on the straight track is regularly variable and fluctuates within a certain range, which will significantly affect the dynamic performance of the rolling stock. It can be drawn from Section 2.3 that the rail cant range is from 1/70–1/10 in actual track. Besides, the variation of wheel-rail contact friction factor is also considered, whose calculation scope is generally between $0.15 \sim 0.5$. The lateral ride comfort index of the locomotives corresponding to four clusters with the variation of rail cant and friction factor is calculated as shown in Figure 13, where the running speed is set to 160 km/h. Besides, the colour of the curve in the Figure also indicates the lateral ride comfort index, and the darker the colour, the smaller the value of lateral ride comfort index, which means the lateral ride comfort of the locomotive is better.

The wheel-rail contact friction factor has negligible influence on the lateral ride comfort, but the rail cant has a significant influence on the lateral ride comfort, especially when the value of rail cant is large, which is consistent with the influence law of rail cant on equivalent conicity in Figure 3. The rail cant variation alters the equivalent conicity, thereby affecting the lateral ride comfort of the high-speed locomotive. Regarding the locomotive employing the parameter combination of Cluster 18th, the lateral ride comfort yields to larger changes with the variation of rail cant, which means that the corresponding rail cant robustness of lateral ride comfort is poor. However, when the high-speed locomotive adopts the parameter combination of the other three clusters, the rail cant robustness is better. It can be deduced that the rail cant robustness of the locomotive employing the parameter combination of Type *Large* is poor, but the rail cant robustness is good when the parameter combination of Type *Small* or Type *Medium* is adopted.

6. Conclusions

(1) This paper conducts the Stability/Comfort optimisation for the high-speed electric locomotive (Bo-Bo) by means of the genetic algorithm NSGA-II. The Pareto frontier of multi-objective optimisation shows that the linear stabilities under low-conicity and high-conicity conditions are contradictory, and the low-conicity stability has a strong positive correlation with the lateral ride comfort under the low-conicity condition.

(2) Through observing the distribution of six key suspension parameters and implementing global sensitivity analysis with regard to the Pareto frontier data, the reasonable value ranges of suspension parameters are obtained. Besides, the three suspension parameters including the primary longitudinal stiffness *kpx*, the primary lateral stiffness *kpy* and the secondary lateral damper series stiffness *kncsy*, have no obvious influence on the locomotive lateral dynamic performance within the optimised scope. Nevertheless, there is a certain matching relationship between the damping of yaw damper *csx*, the damping of the secondary lateral damper *csy* and the yaw damper series stiffness *kncsx*, and the combination mode of three parameters has a greater impact on the lateral stability and ride comfort of the high-speed locomotive.

(3) According to the combination mode of the *csx*, *csy* and *kncsx*, three types of parameter combinations are proposed, which are Type *Small*, Type *Medium* and Type *Large*, and the three objective performance characteristics of each parameter combination type are summarised. Besides, the speed robustness and rail cant robustness regarding the three parameter combination types are also analyzed. When the high-speed locomotive employs the Type *Medium*, both the speed robustness and rail cant robustness are good, and the stabilities under low-conicity and high-conicity condition and lateral ride comfort can be all satisfied. Therefore, the parameter combination of Type *Medium* should be employed in the design of high-speed locomotives.

Disclosure statement

No potential conflict of interest was reported by the author(s).

Funding

The material in this paper is based on work supported by grants (51675443, 51735012) from the National Natural Science Foundation of China, National Railway Group Science and Technology Program [Grand Number N2020J026], National Science and Technology Support Program [Grand Number2018YFB1201703], and Traction Power State Key Laboratory [Grand Numbers No. 2019TPL_Q07, No. 2019TPL_Q08] of the Independent Research and Development Project.

References

[1] Alfi S, Mazzola L, Bruni S. Effect of motor connection on the critical speed of high-speed railway vehicles. Veh Syst Dyn. 2008;46(sup1):201–214.

[2] Ken H. Jane' s world railways. UK: Jane's Information Group; 2001.

[3] Yao Y, Wu GS, Sardahi Y, et al. Hunting stability analysis of high-speed train bogie under the frame lateral vibration active control. Veh Syst Dyn. 2018;56(2):297–318.

[4] Yao Y, Li G, Sardahi Y, et al. Stability enhancement of a high-speed train bogie using active mass inertial actuators. Veh Syst Dyn. 2019;57(3):389–407.

[5] Zhang XX, Wu GS, Li G, et al. Actuator optimal placement studies of high-speed power bogie for active hunting stability. Veh Syst Dyn. 2020;58(1):108–122.

[6] Wei X, Zhu M, Jia L. A semi-active control suspension system for railway vehicles with magnetorheological fluid dampers. Veh. Syst. Dyn. 2016;54(7):982–1003.

[7] Pearson J, Goodall RM, Mei TX, et al. Design and experimental implementation of an active stability system for a high speed bogie. Veh. Syst. Dyn. 2004;41:43–52.

[8] Abood K, Khan RA. Investigation to improve hunting stability of railway carriage using semi-active longitudinal primary stiffness suspension. J Mech Eng Res. 2010;2(5):97–105.

[9] Persson R, Goodall RM, Sasak K. Carbody tilting–technologies and benefits. Veh Syst Dyn. 2009;47(8):949–981.

[10] Suarez B, Mera JM, Martinez ML, et al. Assessment of the influence of the elastic properties of rail vehicle suspensions on safety, ride quality and track fatigue. Veh Syst Dyn. 2013;51(2):280–300.

[11] He YP, Mcphee J. Multidisciplinary optimization of multibody systems with application to the design of rail vehicles. Multibody Syst Dyn. 2005;14(2):111–135.

[12] Masoud M, Mohammad AR. Multi objective optimization of aerodynamic design of high speed railway windbreaks using lattice boltzmann method and wind tunnel test results. Int J Rail Transp. 2018;6(3):183–201.

[13] Peng Y, Hou L, Che QW, et al. Multi-objective robust optimization design of a front-end underframe structure for a high-speed train. Eng Optimiz. 2019;51(5):753–774.

[14] Goldberg DE. Genetic algorithms in search, optimization, and machine learning. Massachusetts: Addison-Wesley Professional; 1989.

[15] Johnsson A, Berbyuk V, Enelund M. Pareto optimisation of railway bogie suspension damping to enhance safety and comfort. Veh Syst Dyn. 2012;50(9):1379–1407.

[16] He YP, McPhee J. Optimization of the lateral stability of rail vehicles. Veh Syst Dyn. 2002;38(5):361–390.

[17] He YP, McPhee J. Optimization of curving performance of rail vehicles. Veh Syst Dyn. 2005;43(12):895–923.

[18] Bideleh SMM, Berbyuk V, Persson R. Wear/comfort Pareto optimisation of bogie suspension. Veh Syst Dyn. 2016;54(8):1053–1076.

[19] Bideleh SMM, Berbyuk V. Multiobjective optimisation of bogie suspension to boost speed on curves. Veh Syst Dyn. 2016;54(1):58–85.

[20] Bideleh SMM, Berbyuk V. Global sensitivity analysis of bogie dynamics with respect to suspension components. Multibody Syst Dyn. 2016;37(2):145–174.

[21] Yao Y, Li G, Wu GS, et al. Suspension parameters optimum of high-speed train bogie for hunting stability robustness. Int J Rail Transp. 2019;8(3):195–214.

[22] Chen XW, Yao Y, Shen LJ, et al. Multi-objective optimization of high-speed train suspension parameters for improving hunting stability. Int J Rail Transp. 2021. doi:10.1080/23248378.2021.1904444.

[23] SIMPACK 2018 Documentation. Dassault Systemes Simulia Corp, France; 2017.

[24] Kalker JJ. A fast algorithm for the simplified theory of rolling contact. Veh Syst Dyn. 1982;11:1–13.

[25] Li JY, Liu LY, Kou DH. Wu Guang high-speed rail track irregularity power spectrum analysis. Appl Mech Mater. 2014;638–640:1224–1228.

[26] Pombo J, Ambrósio J, Silva M. A new wheel–rail contact model for railway dynamics. Veh Syst Dyn. 2007;45(2):165–189.
[27] Sun JF, Chi MR, Jin XS, et al. Experimental and numerical study on carbody hunting of electric locomotive induced by low wheel–rail contact conicity. Veh Syst Dyn. 2021;59(2):203–223.
[28] Iwnicki S. Handbook of railway vehicle dynamic. New York: CRC/Taylor & Francis Group; 2006.
[29] Pombo J, Ambrósio J. An alternative method to include track irregularities in railway vehicle dynamic analyses. Nonlinear Dyn. 2012;68:161–176.
[30] Polach O. On non-linear methods of bogie stability assessment using computer simulations. Proc IMechE Part F: J Rai Rapid Transit. 2006;220(1):13–27.
[31] Polach O. Comparability of the non-linear and linearized stability assessment during railway vehicle design. Veh Syst Dyn. 2006;44(sup1):129–138.
[32] GB/T5599. Specification for dynamic performance assessment and testing verification of rolling stock. National Railway Administration, China; 2019.
[33] Huang CH, Zeng J, Liang SL. Carbody hunting investigation of a high speed passenger car. J Mech Sci Technol. 2013;27(8):2283–2292.
[34] Iooss B, Lemaître P. A review on global sensitivity analysis methods. In: Dellino G, Meloni C, editors. Uncertainty management in simulation-optimization of complex systems, operations research/computer science interfaces series. New York: Springer; 2015. p. 101–122.
[35] Nossent J, Elsen P, Bauwens W. Sobol' sensitivity analysis of a complex environmental model. Environ Modell Softw. 2011;26(12):1515–1525.
[36] Anderson TW. An introduction to multivariate statistical analysis. 3rd edn Hoboken: John Wiley & Sons; 2003.
[37] Xia F, True H. On the dynamics of the three-piece-freight truck. Proceedings of the 2003 IEEOASME joint rail conference; 22-24 April, 2003; Chicago, IL.